Table VIII
List of Observed Frequencies (cm^{-1}) for Crystalline Samples of ITPP-d_8 at Two Different Temperatures and of ITPP-d_2 at Room Temperature[a]

polypentadiene-d_2 room temp	polypentadiene-d_8 room temp	polypentadiene-d_8 liq N_2 temp
198 w	280 w	
300 w	392 m	392 m
433 m	422 m	422 m
452 m	470 vw	471 w
515 vw	647 w	648 m
705 m	692 vw	692 m
792 m	720 vs	725 vs
836 w	746 vs	748 vs
850 vw	764 s	765 vs
883 w	800 vw	804 vw
928 vs	818 m	819 s
950 vs	882 m	883 m
970 vs	901 m	902 s
1041 s	909 s	911 s
1053 vw	935 vw	936 w
1079 m	954 m	957 s
1110 w	1006 vw	1006 w
1126 s	1035 m	1039 m
1160 w	1045 s	1045 s
1244 m	1055 vs	1052 vs
1260 vw		1057 vs
1293 m	1060 vs	1060 vs
1310 vw		1065 vs
1335 m	1078 vw	1080 vw
1370 s	1100 w	1104 m
1450 vs	1139 s	1142 s
1455 vs	1175 w	1180 w
	1200 vw	1203 vw
	1286 vw	1286 vw

[a] vw = very weak, w = weak, m = medium, s = strong, vs = very strong.

placement about the chain axis and of three translations for each repeat unit.

The crystal field also modifies the description of all other low-lying vibrational modes related to modes with nonzero frequency for the isolated chain and in some case consistently affects the calculated value. In this respect it is interesting to note that a frequency calculated at 211 cm^{-1} for the single chain of ITPP is now shifted, by the interchain potential, to 230 cm^{-1}. This calculated frequency was not considered characteristic of the chain conformation, as its value is not very sensitive to chain geometry, and was the only one for which a rather large error occurred for both possible chain models. The better fit between calculated and observed values obtained after the inclusion of interchain potential confirms the validity of the calculations and of the internal and external potential adopted in this paper. Although it is not possible to draw conclusions on the crystal structure of ITPP, normal-mode calculations including interchain terms show that the vibrational spectrum cannot be satisfactorily reproduced by using the results of the X-ray analysis,[7] while a good fit occurs for a crystal geometry based on a skew conformation of each polymer chain.

References and Notes

(1) N. Neto, M. Muniz-Miranda, E. Benedetti, F. Garruto, and M. Aglietto, *Macromolecules*, preceding paper in this issue.
(2) N. Neto and C. Di Lauro, *Eur. Polym. J.*, 3, 645 (1967).
(3) P. Bardi, Thesis, University of Pisa, 1974.
(4) L. Lani, Thesis, University of Pisa, 1972.
(5) M. Kobayashi, *J. Chem. Phys.*, 70, 4797 (1979).
(6) N. Neto and D. Kirin, *Chem. Phys.*, 44, 245 (1979).
(7) I. W. Bassi, G. Allegra, and R. Scordamaglia, *Macromolecules*, 4, 575 (1971).
(8) D. E. Williams, *J. Chem. Phys.*, 47, 4680 (1967).
(9) S. L. Hsu, W. H. Moore, and S. Krimm, *J. Appl. Phys.*, 46, 4185 (1975).

Notes

Chiral Discrimination in Poly(α-amino acid)–Metal Complexes

M. DENTINI and P. De SANTIS*

Istituto di Chimica Fisica, Università di Roma, Roma, Italy

M. SAVINO

Centro di Studio per gli Acidi Nucleici del CNR Istituto di Fisiologia Generale, Università di Roma, Roma, Italy.

Received April 18, 1979

The conformational order and rigidity that generally characterize the state of poly(α-amino acids) in solution and their intrinsic chirality provide a unique opportunity for investigating topochemical effects such as stereospecificity and stereoselectivity in reactions occurring on such protein-like matrices. In fact, polypeptide systems having functional side chains are capable of stereospecifically binding square-planar prochiral metal complexes at pairs of amino acid residues along the chain.[1-3]

We report our CD and ESR investigations of the influence of chiral and conformationally rigid polypeptide matrices on the structure of anchored metal complexes. The right-hand side of Figure 1 illustrates the polypeptide matrices used. These are bound via Schiff bases of salicylaldehyde or pyridoxal with ornithine and lysine side

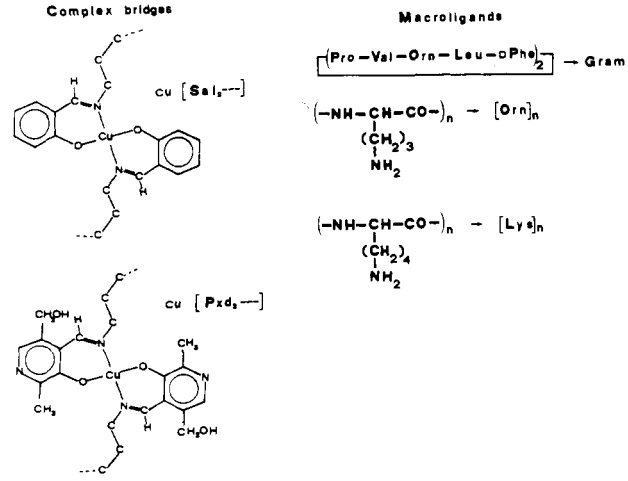

Figure 1. Macroligands (right) and complex bridges (left) investigated.

chains; the complex bridges are indicated on the left-hand side.

Under the experimental conditions adopted (room temperature; methanol, trifluoroethanol [apparent pH 7], chloroform, *N*,*N*-dimethylformamide [DMF], and trimethyl phosphate [TMP] organic solvents) the confor-

0024-9297/80/2213-1308$01.00/0

Table I
Electron Paramagnetic Resonance Parameters of Copper(II) Macrocomplexes at 77 K

macrocomplex	solvent	$g_\parallel$	10^4A, cm^{-1}
$[Cu(Sal)(Lys)]_n$	MeOH	2.24	174
$[Cu(Pxd)(Orn)]_n$	MeOH	2.24	180
$Cu(Sal)_2(Gram)$	MeOH	2.24	173
$Cu(Pxd)_2(Gram)$	$CHCl_3$	2.23	172
$Cu(Pxd)_2(Gram)$	MeOH	2.25	180
$Cu(Pxd)_2(Gram)$	DMF	2.24	188

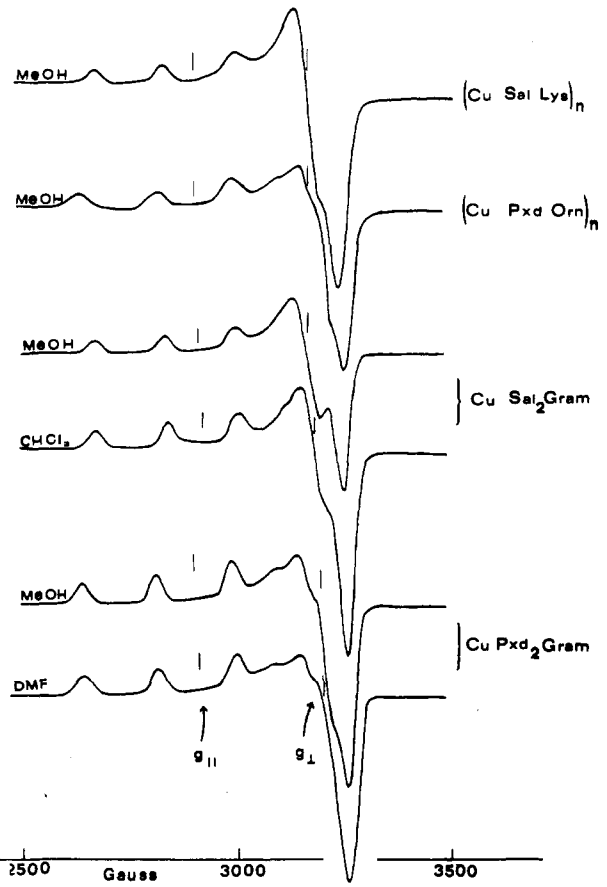

Figure 2. ESR spectra of $[Cu(Sal)(Lys)]_n$ and $[Cu(Pxd)(Orn)]_n$ in methanol, of $Cu(Sal)_2(Gram)$ in methanol and chloroform, and of $Cu(Pxd)_2(Gram)$ in methanol and *N,N*-dimethylformamide. The solutions were 1×10^{-3} M in Cu(II) and 8×10^{-3} M in lysine or ornithine residues.

mations of the polypeptides are stabilized as right-handed α helices in the cases of polyornithine and polylysine and as the antiparallel β sheet in the case of the natural cyclodecapeptide Gramicidin S. Therefore, these polypeptides represent, under the same physicochemical conditions, the secondary structures found in proteins.

In all cases, the visible regions show poorly resolved d–d bands with molar extinction coefficients not exceeding ~50, suggesting trans square-planar coordination of copper ion. This assignment is supported by ESR spectra (Figure 2). In fact, similar trends characterize the different macrocomplexes even when the solvents are changed. The $g_\parallel$ values and hyperfine coupling constants are typical of square-planar Cu(II) complexes (see Table I).

In spite of this general pattern of similarity, we have previously shown[1-3] that the CD spectra are very different, on account of their higher degree of structural sensitivity. The CD spectra of copper(II) salicylaldimine complexes of polylysine and polyornithine show opposite Cotton effects for all the ligand and copper transitions, despite the fact that all the amino acids are of the L configuration and, in both cases, the polypeptide backbone assumes the

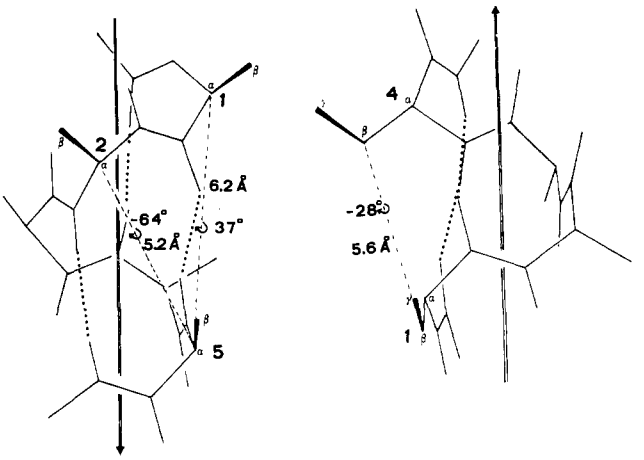

Figure 3. Geometrical features of the right-handed α helix. The helicity of the junctions of the complex bridge to the backbone is emphasized.

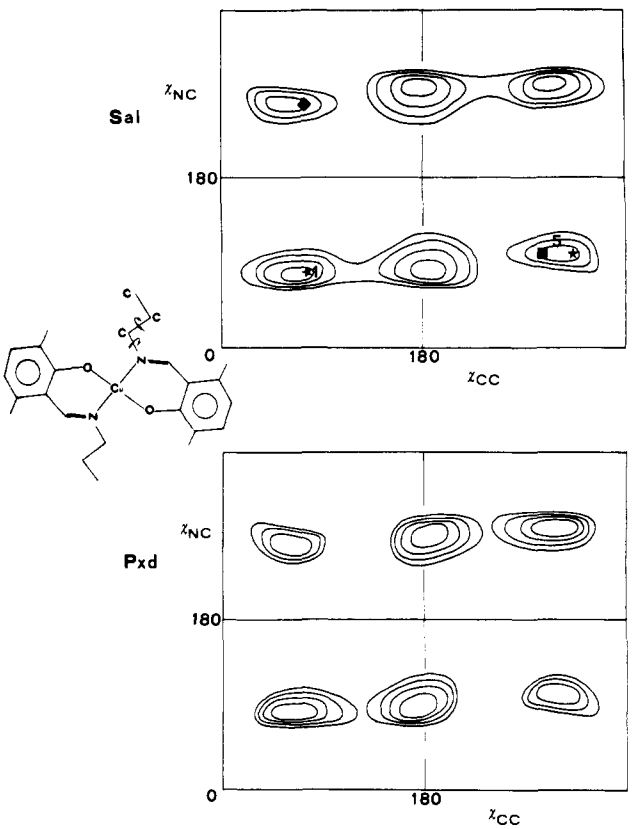

Figure 4. Conformational energy diagrams of the copper(II) salicylaldimine bridge (top) and the copper(II) pyridoxaldimine bridge (bottom) anchored to the macromolecular ligands in terms of the rotation angles χ_{NC} and χ_{CC} for the $N-CH_2$ and CH_2-CH_2 bonds. Contour lines are drawn at intervals of 1 kcal/mol.

right-handed α helix. Similar results were obtained in the case of homologous complexes of the pyridoxaldimine derivatives.[2] An almost perfect inversion of the CD bands extends over the whole range of frequencies, except for the peptide region, which retains behavior typical of the right-handed α-helical conformation.

Replacing methanol by DMF as solvent does not cause a significant modification of the CD spectra of the α-helical complexes. On the other hand, in the binding of the complexes to Gramicidin S, which is stabilized in the antiparallel β-sheet conformation, a peculiar solvent effect takes place in that the two solvents are able to produce a sort of chiral discrimination in the formation of diastereoisomeric complexes.[4] The two spectra have opposite dichroism bands over the whole range of frequencies except

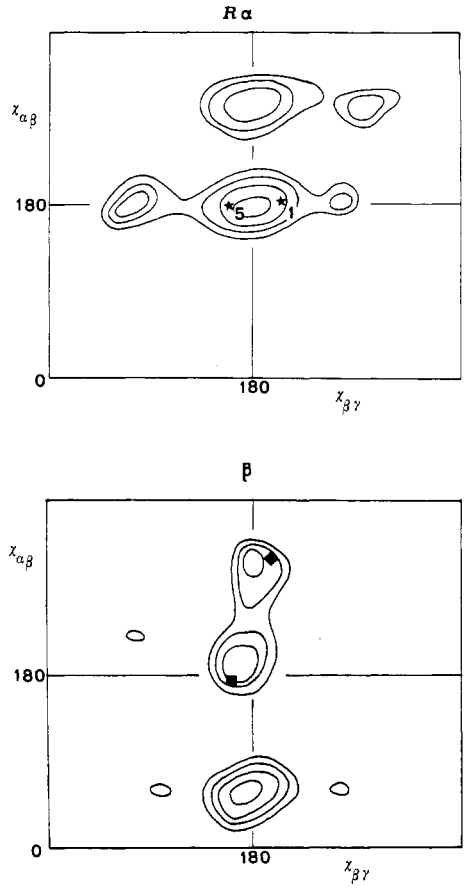

Figure 5. Conformational energy diagrams of the dipeptide residues fixed in the right-handed α helix (top) and in the β-sheet conformation (bottom) in terms of the rotation angles $\chi_{\alpha\beta}$ and $\chi_{\beta\gamma}$ for the side-chain bonds C_α–C_β and C_β–C_γ. Contour lines are drawn at intervals of 1 kcal/mol.

for the peptide transitions, which retain the main features of the Gramicidin S CD spectrum.

This effect is rather general for other pairs of solvents belonging to two classes: alcohols and nonhydroxylated solvents. This solvent effect, which characterizes the copper(II) bis(salicylaldimine) derivatives of Gramicidin S, is absent in the case of homologous complexes of pyridoxaldimine. The CD spectra in methanol and DMF[5] are rather similar.

Conformational Analysis

In order to explain these results, we have investigated by methods of theoretical conformational analysis[6] the geometrical and conformational constraints which control the binding of the complexes to the polypeptides. Figure 3 shows some relevant geometrical features of the right-handed α helix. In particular, the helicity of the junctions available for binding of the complex to the polypeptide backbone is emphasized. These correspond to the C_α–C_β bonds of the first and the fifth (or the fourth) amino acid residues, indicated as 1–5 or 1–4 positions, respectively. To a first approximation, the two situations have opposite helicities and distances. As will be seen below, the 1–5 bridge in polyornithine complexes is the most sterically favorable because it avoids both eclipsed conformations along the hydrocarbon chains and disallowed contacts between nonbonded atoms.

If, however, a CH_2 group is added to each of the junctions at the 1–4 positions in the most stable staggered conformation (see right side of Figure 3), the helicity of the new junctions (corresponding to C_β–C_γ bonds) becomes nearly opposite to that of the 1–5 bridge (left side of Figure 3). Therefore, enantiomeric conformations of the complex bridge will bind at the positions 1–5 in the case of polyornithine and at the positions 1–4 if a CH_2 is added to each of the side chains. This formally changes the polyornithine into the polylysine complexes and basically explains why opposite Cotton effects are observed.

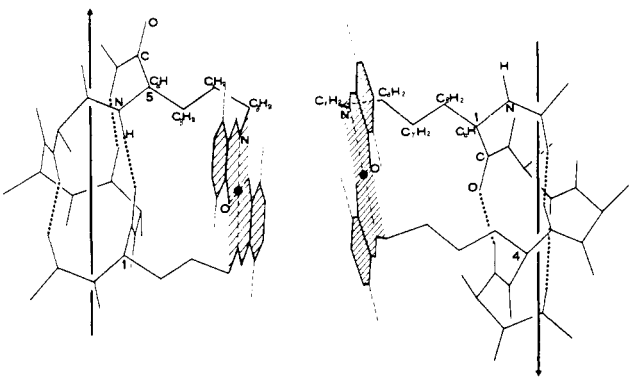

Figure 6. Local structures of the (a) polyornithine and (b) polylysine complexes.

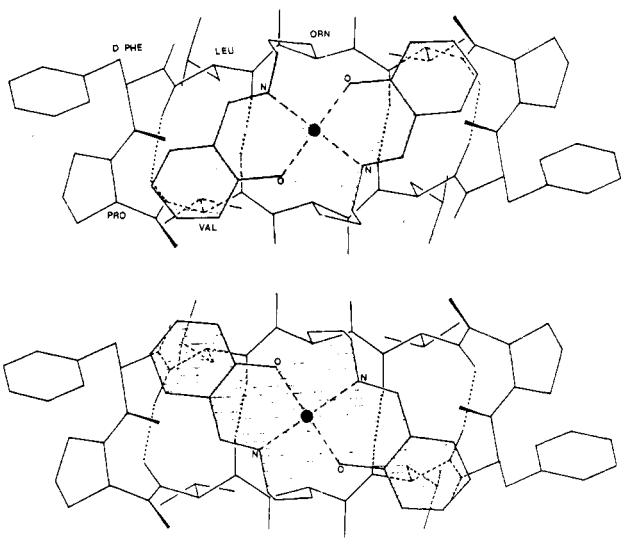

Figure 7. Schematic drawings of the $Cu(Sal)_2$(Gram) diastereoisomeric structures: (top) stabilized in hydroxylated solvents (ethanol, trifluoroethanol); (bottom) in other solvents (chloroform, *N*,*N*-dimethylformamide, trimethyl phosphate, pyridine).

In the case of Gramicidin S, schematically represented in Figure 7, the virtual lack of helicity at the junctions with the complex (the C_α–C_β bonds of the ornithine residues), which generally characterizes the β-sheet structures, does not allow (to a first approximation) ready discrimination of the enantiomeric conformations of the complex bridge. Indeed, in contrast to polyornithine and polylysine, Gramicidin S gives rise to both the diastereoisomeric complexes when the solvent is changed, as evidenced by the inversion of CD bands.

In order to provide further support for this explanation, we investigated the structures of the macrocomplexes by using conformational energy calculations based on a set of van der Waals and torsional potential functions.[6] The most stable conformations of the salicylaldimine and pyridoxaldimine complex bridges were selected by locating the deepest minima in the pertinent energy diagrams in terms of the rotation angles χ_{NC} and χ_{CC} for the bonds N–C and C–C, as represented in Figure 4. The contour lines were drawn at regular intervals of 1 kcal/mol and represent the conformational energy of a half complex bridge.

Because of the absence of interactions between the hydrocarbon chains in the structures of interest, the conformational energy can be easily evaluated as the sum of

the energies of the corresponding pairs of representative points of the two hydrocarbon chain conformations in Figure 4. Therefore, a pair of points in the diagram represents the stability of a given conformation of the complex and determines implicitly the distance between the terminal carbon atoms. In the case of polyornithine, these coincide with the C_β atoms (C_γ for polylysine); the distance between these atoms can assume only the fixed values pertinent to the backbone conformations of the poly(α-amino acid). This, together with the energy, strongly limits the possible conformations of the macrocomplexes.

The conformation represented by the pair of stars in Figure 4 and corresponding to the 1–5 bridge is by far the most favorable in the case of the α-helical polyornithine complex. Moreover, only in this case do the angles of rotations near the peptide backbone, $\chi_{\alpha\beta}$ and $\chi_{\beta\gamma}$, which satisfy the definition of the macrocomplex structure in terms of torsional angles, occur in the deepest energy minima of the diagram in Figure 5, top. Here, the conformational energy of a dipeptide residue having the peptide skeleton conformation fixed in the right-handed α helix is shown in terms of the two rotation angles $\chi_{\alpha\beta}$ and $\chi_{\beta\gamma}$ for the side-chain bonds C_α–C_β and C_β–C_γ, respectively.

In the case of the pyridoxaldimine bridge, the similarity of the energy diagram with that of the salicylaldimine bridge leads to the same conclusions (see Figure 4).

Figure 5, bottom, illustrates the case of the β conformation of the backbone relevant for Gramicidin S, where the presence of the dyad axis almost parallel to the two junctions to ornithine allows the two enantiomeric complexes with conformationally equivalent hydrocarbon chains to be bound to the polypeptide matrix. The resulting two diastereoisomeric complexes are represented by different figures on the energy diagrams in Figure 4 and Figure 5, bottom.

Discussion and Conclusions

Figure 6 illustrates the local structure of the polyornithine and polylysine complexes. The two diastereotopic faces of the square-planar copper complex are alternately anchored to the positions 1–5 and 1–4, respectively, for polyornithine and polylysine. In the latter case, the longer hydrocarbon side chain allows a higher degree of conformational flexibility.

Figure 7 illustrates the proposed structures of diastereoisomeric copper(II) salicylaldimine complexes of Gramicidin S. In contrast to helical macrocomplexes, the Gramicidin S molecule (or β-sheet polypeptide conformations in general) extend over the whole length of the square-planar complex so that side effects could arise. These effects are amplified by differential solvation of the macromolecular surface. In fact, solvents preferentially solvating the carbonyl groups (eclipsed by the benzene rings in the upper diastereoisomer), such as methanol and trifluoroethanol, stabilize the lower conformation in Figure 7, whereas solvents such as chloroform, DMF, and TMP stabilize the upper diastereoisomeric configuration. This effect is absent in the case of Gramicidin S complexes of pyridoxaldimine, where one of the two diastereoisomers is stabilized on account of possible hydrogen bonds between the pyridoxaldimine CH_2OH group and the amide C=O group of D-phenylalanine residues, as model building suggests.

As a general conclusion, ordered polypeptide matrices are capable of reacting stereospecifically with square-planar copper complexes because of the intrinsic chirality of their binding surfaces. Such chiral discrimination can be amplified by cooperative as well by differential solvation effects.

Acknowledgment. Financial support by CNR is gratefully acknowledged. We are indebted to Professor D. Cordischi for useful discussions concerning the ESR measurements.

References and Notes

(1) Dentini, M.; De Santis, P.; Savino, M.; Verdini, A. *Makromol. Chem.* **1974**, *175*, 327.
(2) Dentini, M.; De Santis, P.; Savino, M.; Verdini, A. *Biopolymers* **1978**, *17*, 909.
(3) De Santis, P. *Chim. Ind. (Milan)* **1976**, *58*, 626.
(4) De Santis, P.; D'Ilario, L.; La Manna, G.; Morosetti, S.; Savino, M. *Biopolymers* **1973**, *12*, 423.
(5) Dentini, M.; De Santis, P.; Savino, M., unpublished results.
(6) De Santis, P.; Liquori, A. M. *Biopolymers* **1971**, *10*, 699.

Effect of Urea on the Intrinsic Viscosity of Randomly Coiled Poly(α-L-glutamate)[1a]

JEFFREY SKOLNICK[1b] and ALFRED HOLTZER*[1c]

Departments of Chemistry, Washington University, St. Louis, Missouri 63130, and Louisiana State University, Baton Rouge, Louisiana 70803. *Received March 25, 1980*

Use of urea as a denaturant for proteins is widespread, and there is enormous interest in the precise mode by which it exerts this action. Since there is also a sizable literature on the use of water-soluble synthetic polypeptides as model substances for proteins, it would be expected that the effect of urea on the physical properties of the most thoroughly investigated polypeptide, poly(α-L-glutamate) [abbreviated $(Glu)_n$] would long since have been exhaustively delineated. This appears not to be the case; indeed, although the influence of urea on the helix–coil transition has been studied by the titration method and found, as expected, to favor the random coil form,[2] very few measurements of other physical properties came to light in our literature search.

Since one important hypothesis on the molecular basis for urea's denaturing action holds that it denatures by virtue of a strong, attractive interaction with the exposed peptide groups in the random coil form of a protein or polypeptide,[3] it seemed to us that the intrinsic viscosity (being notoriously sensitive to molecular dimensions of random coils) of $(Glu)_n$ random coils would be strongly influenced by urea. We report such measurements here. The results are surprising.

Materials and Methods

Unless otherwise indicated, all experimental details were as described earlier.[4,5] Baker reagent grade urea was recrystallized from ethanol. The sample of $(Glu)_n$ was purchased from Sigma Chemical Co. Measurement of its intrinsic viscosity at pH 7.1 in 0.1 M NaCl at 25.5 °C and use of the earlier calibration[5] showed it to have a weight-average molecular weight of 77 500. A thorough study of its intrinsic viscosity vs. salt (NaCl) concentration at pH 7.1 showed a dependence that is in quantitative agreement with the relationship found earlier.[5] Each individual intrinsic viscosity was determined by fitting measurements of η_{sp}/c at at least five concentrations (g dL^{-1}) to the usual equation $\eta_{sp}/c = [\eta] + k'[\eta]^2c$. Dialysate was always used as solvent. Media of two very different ionic strengths were used; both were buffered at pH 7.1 with a mixture of Na_2HPO_4 and NaH_2PO_4. In detail, these two media were (in addition to any urea present)[6] $(NaCl)_{0.1}(NaP_i)_{0.01}(7.1)$ and $(NaCl)_{3.0}(NaP_i)_{0.01}(7.1)$. The temperature was 25.50 ± 0.01 °C for all.

Results and Discussion

The experimental findings are summarized in Figure 1 as a plot of intrinsic viscosity (dL g^{-1}) vs. molarity of urea.

0024-9297/80/2213-1311$01.00/0